



ELSEVIER

Available online at www.sciencedirect.com

SCIENCE @ DIRECT®

Journal of Applied Geophysics 54 (2003) 111–125

JOURNAL OF
APPLIED
GEOPHYSICS

www.elsevier.com/locate/jappgeo

Implications of magnetic backgrounds for unexploded ordnance detection

Dwain K. Butler*

Alion Science and Technology Corporation, U.S. Army Engineer Research and Development Center, 3909 Halls Ferry Road, Vicksburg, MS 39180-6199, USA

Received 8 February 2002; accepted 26 August 2003

Abstract

Detection of buried unexploded ordnance (UXO) requires application of geophysical methods that exploit contrasts in magnetic susceptibility and/or electrical conductivity of the UXO relative to surrounding soil and rock (the geologic background). At many sites, the contrasts are very large, and the detection capability is relatively independent of the geologic background. Some sites, however, are predictably problematic, such as volcanic terrains (e.g., Maui and Kaho'olawe, HI, USA). Other sites that would not intuitively be predicted to pose detection problems are found to have localized high susceptibility zones with wavelengths and magnitudes that can significantly complicate UXO detection. Details of a site in Indiana (USA) are presented that illustrate order of magnitude variation of magnetic susceptibility over distances of 2–3 m. Magnetic susceptibility at the site correlates to topography and soil type. Magnetic power spectral density plots from magnetic surveys at selected areas at the Indiana site are compared to each other and to data from Maui, HI, and demonstrate the key issues in UXO detection with magnetometry. Magnetic susceptibility data from Kaho'olawe are used to illustrate the effects on electromagnetic induction surveys for UXO detection and discrimination. The phenomenological observations suggest approaches for magnetic and electromagnetic induction survey data processing to enhance anomaly detectability and model-based inversion.

© 2003 Elsevier B.V. All rights reserved.

Keywords: Magnetic susceptibility; Unexploded ordnance; Detection and discrimination

1. Background

Unexploded ordnance (UXO) cleanup or remediation is currently the highest priority military environmental quality requirement in the United States (U.S.) at active training and testing ranges, at military sites scheduled for closure, and at formerly used

military sites. Key features of the UXO problem in the U.S. are: (a) millions of hectares of land potentially contaminated with UXO; (b) hundreds of sites and locations; (c) extremely diverse geologic and environmental conditions; (d) UXO at the surface and buried to depths as great as 10 m; (e) UXO sizes from 20-mm projectiles to 2000-lb bombs (see Fig. 1). UXO cleanup requirements of comparable or larger scope exist throughout the world as a legacy of past military conflicts. The UXO cleanup problem as discussed in this paper is totally distinct from the landmine clearance problem that is so ubiquitous in

* Tel.: +1-601-634-2127.

E-mail address: Dwain.K.Butler@erd.c.usace.army.mil (D.K. Butler).

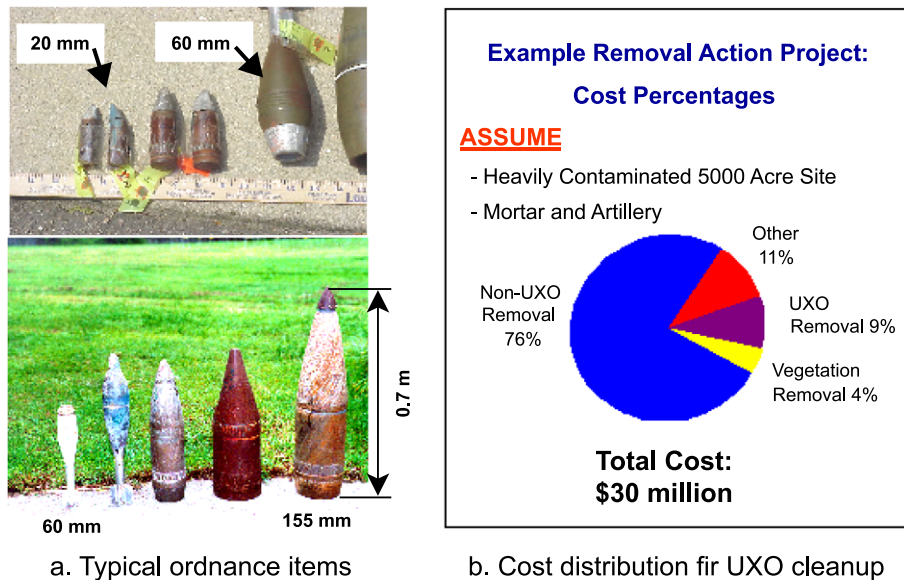


Fig. 1. (a) Typical ordnance items and (b) cost distribution for hypothetical UXO cleanup scenario (5000 acres to 2023 ha; cost in USD).

occurrence and importance throughout the world (Butler, 1997).

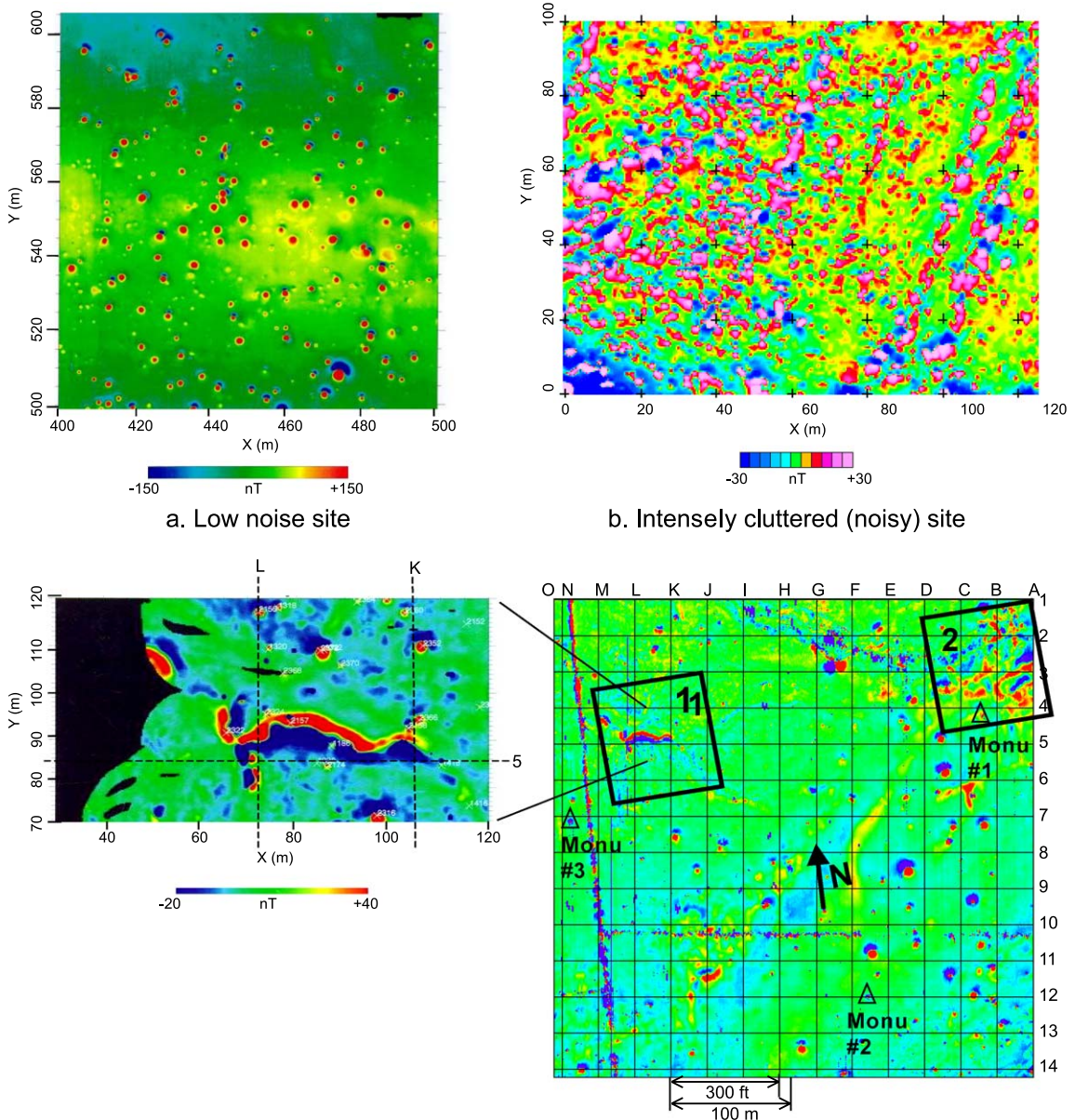
The task of UXO cleanup over large areas is technically challenging and problematic. At many sites, buried UXO are routinely *detected* by sensor sweeps or geophysical surveys, relative to the site-specific background (geologic background and cultural clutter). However, there is no general capability to effectively *discriminate* UXO geophysical anomalies from false alarm anomalies; and UXO type cannot be identified with specificity from remotely sensed data. The probability of UXO detection on documented test sites can exceed 90% for carefully executed geophysical surveys; however, even for the best performers, the false alarm rates (i.e., the number of non-UXO targets that must be excavated for each UXO item found) remain quite high (from 10's to 100's depending on site specific conditions). Without discrimination capability, large numbers of false alarm anomalies must be investigated, with 75% or more of the cleanup cost spent on excavating false alarm sources (Fig. 1). Additional technical challenges relate to the requirement for extremely high-resolution, high-fidelity data acquisition. The examples shown in this paper are some of the highest resolution geophysical field datasets ever obtained (e.g., total field magnetic data with 25-cm line spacing and

nominal 10-cm measurements along lines; see Fig. 2). Concomitant with the requirements for measurement density and the resulting large data volume management are exacting positioning and navigation capability for data acquisition and for subsequent relocation of target anomalies.

2. Geophysical methods for UXO surveys

The most frequently used methods for UXO location surveys are total field magnetometers (TFM) and "simple" time domain electromagnetic induction (TDEM) instruments. "Simple" TDEM systems loosely refer to systems that measure one or two time windows (gates) from the induced transient decay signal. Application of these systems by *experienced geophysical practitioners* during demonstrations at controlled UXO test sites achieves probabilities of detection of UXO in excess of 90% (e.g., Pederson and Stalcup, 1997). Generally, for production surveys at large sites, only one of these systems will be deployed.

Other geophysical methods proposed, demonstrated, and/or utilized for UXO surveys are ground penetrating radar (GPR), frequency domain electromagnetic induction (FDEM) systems, multi-gate



c. Site with prominent geologic magnetic anomalies, Jefferson Proving Ground, Indiana

Fig. 2. Total magnetic field maps for sites with three distinct magnetic background conditions.

TDEM systems, multi-component TDEM systems, multi-component (vector) magnetometers, magnetic gradiometers, acoustic/seismic methods, gravimetry, and airborne systems of various types. Acoustic/seismic and gravimetry methods have only limited or niche applicability in UXO surveys (Butler, 2001;

Butler et al., 2001). GPR is not an applicable tool for large area UXO detection surveys, although it has potential applicability for small area UXO discrimination and identification efforts, where the UXO are located by other survey methods. Efforts to apply airborne geophysical surveys for UXO location at

sensor heights typically greater than 25 m, including magnetometry, GPR, and SAR, have been failures. Recently, however, TFM and simple TDEM surveys from a helicopter platform at 1.0–2.0 m sensor elevation have shown promise for large area UXO detection surveys, detecting areas of UXO concentration, as well as larger individual ordnance items (e.g., Gamey 2001). Multi-gate (25–30 time gates), multi-component TDEM systems and multi-frequency FDEM systems have potential for large area UXO detection surveys, as well as near-real-time discrimination or follow-on small area discrimination of detected anomalies (Butler et al., 1998a,b; Pasion and Oldenburg, 2001; Keiswetter, 2000).

3. Geologic and cultural background considerations for UXO surveys

A common assumption in routine geophysical surveys for location of buried UXO is that the electrical conductivity, dielectric permittivity, and magnetic susceptibility (permeability) of the UXO are much larger than the host medium, i.e., the physical property contrasts are very large. In this case of very large contrasts, location (detection) capability is virtually independent of the physical properties of the host medium. However, there are notable exceptions, and geophysical surveys for UXO can indeed be complicated or severely inhibited by the physical properties of the host medium. Kaho'olawe Island, HI, is an example of a UXO cleanup site where problems would be expected, and where, in practice, high magnetic susceptibility of the host medium makes magnetic surveys for UXO detection virtually impossible and complicates electromagnetic surveys (Khadr et al., 1997; Pasion et al., 2002). The "soils" at Kaho'olawe are derived from a tholeiitic basalt parent rock with up to 20% magnetite. Other sites, where problems would not be anticipated, such as Jefferson Proving Ground (JPG), Indiana, can have significant variability of near-surface magnetic susceptibility (Butler et al., 1999). The nature of physical property variations at JPG, specifically the magnetic susceptibility, is the source for much of the discussion in this paper. The soils at JPG are predominantly very fine, silty sands of glacial origin, with quartz the dominant mineral and only trace amounts of clay.

JPG is the location of a major UXO detection technology demonstration program, conducted in five phases over the period 1994–2001 (e.g., Pederson and Stalcup, 1997; Butler et al., 1998a,b; Cespedes, 2001; Cespedes and Dinh, 2002).

Geophysical sensor responses in UXO surveys are a superposition of the signatures of the host medium, cultural sources, and the buried ordnance. Signatures due to the host medium and cultural sources constitute the *background*. The host medium in most cases is a soil. Part of the response to the host medium will be due to materials (soil and rock) below the depth of burial of the UXO as well as surface topography. Conditions where the nature of the host medium makes buried UXO detection problematic include: soils with high magnetic susceptibility (or with included rocks or shallow "bedrock" with high magnetic susceptibility); high electrical conductivity soils that produce large EM induction responses and attenuate GPR signals after short distances of propagation; soils with large rocks, tree roots, and animal burrows that produce GPR signatures similar in some respects to GPR signatures from UXO; highly heterogeneous soils with large contrasts in magnetic susceptibility, electrical conductivity, and/or dielectric permittivity with size scales comparable to the buried UXO. Two types of cultural sources contribute to sensor responses: (1) objects ("clutter") on or buried in the host medium, such as buildings, fences, exploded ordnance debris and other metallic objects (false alarm sources), and (2) interference signals from power lines and EM transmitters of various types.

Total magnetic field (TMF) anomaly maps for three sites that illustrate some of the range of backgrounds encountered at UXO test sites and cleanup sites are shown in Fig. 2. The three sites all have buried UXO (for test sites, the buried ordnance items are inert, but the terminology UXO is used for simplicity). For the low background noise site (Fig. 2a), the UXO anomalies are readily apparent, and inversion of the anomalies for details of the sources should be straightforward. The intensely cluttered site (Fig. 2b) has so many anomalies due to shallow ferrous objects that even identification of the UXO anomalies is extremely difficult; the remains of buried communication lines cause some of the linear anomaly features. For the JPG site (Fig. 2c), identification of the UXO anomalies becomes problematic when

located in close proximity to or within the larger “geologic” anomalies (area 1) or cultural feature anomalies. There are also some geologic anomalies at the JPG site that are comparable in magnitude and wavelength to UXO anomalies (e.g., area 2). The Phase V demonstration at JPG (ca. 2000–2001) exploited the fact that both areas with “quiet” magnetic backgrounds and areas with prominent geologic magnetic anomalies were present (Cespedes, 2001). Following the Phase V demonstration at JPG, the demonstration moved to a test site established on Kaho’olawe, HI (Cespedes and Dinh, 2002).

4. Magnetic susceptibility: spatial variability

Magnetic susceptibility of near-surface materials does not normally vary significantly over very short distances (e.g., a few meters), particularly in a non-igneous terrain. It is not uncommon, however, for soils to have higher magnetic susceptibilities than the parent rocks due to various geochemical processes during weathering and also selective sorting of heavy minerals (Burger, 1992; Le Borgne, 1955; Mullins, 1977). Magnetic susceptibility of sedimentary rock averages 5×10^{-4} (SI), while for soils derived from sedimentary rocks it can be as high as 1.5×10^{-3} (SI).¹ Soil magnetic susceptibility typically can vary by factors of 2 to 3 over distances of 10’s of meters. Commonly, the susceptibility variation of soils in an area (as portrayed in a histogram of values) will be unimodal with a rather narrow peak (Scollar et al., 1990; Dearing, 1994), and there are intuitive magnetic susceptibility correlations to soil type and well-known correlations to topography. Anomalously high or complex spatial variability of magnetic susceptibility were never anticipated for the JPG sites.

During preparation for and execution of the JPG Phase IV demonstrations, the presence of significant and unexplained magnetic anomalies was indicated by some of the demonstrators, based on their Phase II and III demonstration experience. Fig. 2c is a TMF anomaly map from a Phase III demonstration (McDonald and Nelson, 1999). In addition to mag-

netic anomalies due to buried targets (ordnance and non-ordnance targets), the magnetic map includes other anomalies caused by cultural and geologic sources. An obvious cultural feature anomaly is the linear anomaly pattern that trends nearly due north–south along the western side of the 16-ha (40-acre) site that is caused by an existing fence. Another linear anomaly occurs between east and west grid lines 10 and 11 and is caused by the buried remnants of a fence. The longer wavelength anomalies, many of which are subtle in expression, are geologic in origin and likely from very shallow-origin sources. Two significant anomalous areas, which are not subtle, exist in the northeast and northwest quadrant of the site (Fig. 2c).

5. JPG magnetic susceptibility measurements and observations

5.1. Northwest quadrant magnetic anomaly

Grid lines K and M and grid lines 4 and 6 approximately bound the large magnitude geologic anomaly feature in the northwest quadrant (Fig. 2c). The anomaly coincides with a notable topographic depression associated with surface drainage (Butler et al., 1999). More subtle expressions of the anomaly extend outside this area to the northeast and southwest, following the trends of drainage features. An enlarged view of the magnetic anomaly map of this feature is also shown. Although the overall anomalous feature is complex, the most obvious aspect of the anomaly is a bipolar pattern, with a large magnitude negative band (~ -130 nT) to the south and a large magnitude positive band ($\sim +115$ nT) to the north. Some of the Phase II and III demonstrators expressed the conviction that the prominent anomaly must be due to buried ferrous materials that were not detected during the test site development. However, the relative signs of the anomaly are opposite to that expected for a buried ferrous object; this fact and the relatively sharp definition of the anomaly suggest a shallow, geologic origin.

Two types of measurements were obtained in situ to characterize the nature of the anomalous feature. A frequency domain EM system was used to acquire terrain conductivity and magnetic susceptibility meas-

¹ To convert the volume magnetic susceptibilities used in this paper to mass susceptibilities, divide by the bulk density.

urements (Geonics EM38; McNeill, 1986) over the area bounded by grid lines K, M, 4, and 6 (61×61 -m or 200×200 -ft area.). Measurements were acquired approximately on a 6×2 -m grid for terrain conductivity and on a 6×6 -m grid for magnetic susceptibility. Magnetic susceptibility measurements with the EM38 approximate a depth-weighted, volume-averaged value for the upper 0.5 m of the subsurface. Magnetic susceptibility measurements were also acquired with a laboratory magnetic susceptibility system fitted with a field measurement search coil (Bartington MS2 Magnetic Susceptibility System; Dearing, 1994) on a 6×6 -m grid within the same area as the EM38 measurements. In addition, MS2 measurements were acquired along grid lines K, L, and M at 30-m intervals (100 ft). MS2 magnetic susceptibility measurements approximate volume-averaged values for the upper 10–15 cm of the subsurface. Both EM38 and MS2 measurements are magnitudes of the total, volume magnetic susceptibility.

Results of measurements to investigate the nature of the northwest quadrant magnetic anomaly are presented in Figs. 3 and 4. Significant variation (order of magnitude) in magnetic susceptibility that occurs over horizontal distances less than 10 m are observed in the map of magnetic susceptibility over the anomalous region (Fig. 3). There are no obvious correlations of susceptibility to terrain conductivity (Butler et al., 1999). However, the correlation to the northwest quadrant total magnetic field anomaly in Fig. 2c is obvious. Fig. 4 presents the MS2 magnetic susceptibility measurements along line K and compares them to the EM38 values. The magnetic susceptibility along line K shows a systematic decrease in values from approximately 6×10^{-4} (SI) in the north to approximately 1×10^{-4} (SI) in the south, with anomalous values in the area of the northwest quadrant magnetic anomaly. Both the EM38 and the MS2 values show the same trends in the anomalous area: proceeding from south to north, there is a high-low-high pattern. The trough of the drainage

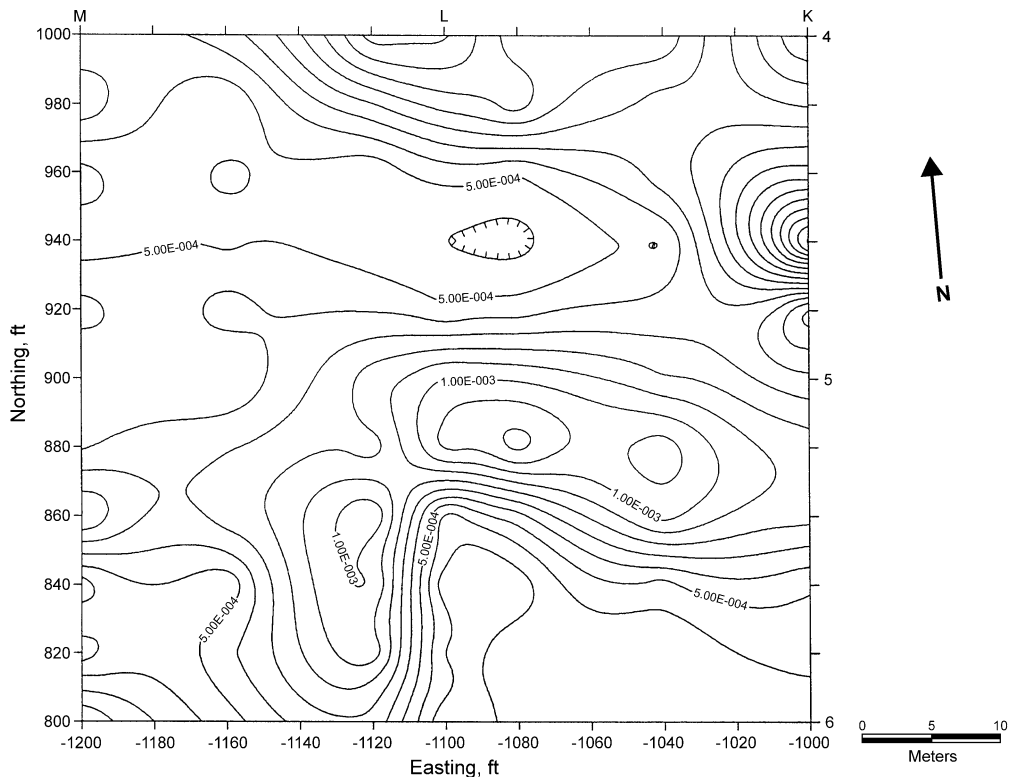


Fig. 3. Magnetic susceptibility map for area of JPG site centered on the prominent geologic magnetic anomaly shown in Fig. 2c.

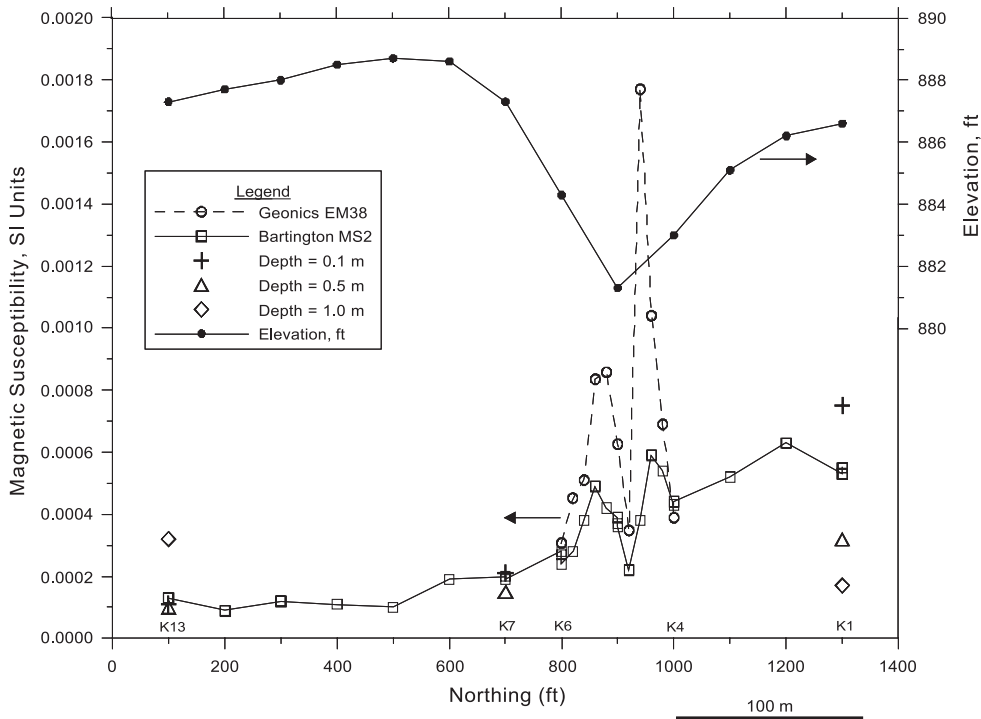


Fig. 4. Magnetic susceptibility measurements and elevation profile along the K-line of the JPG site (see Fig. 2c).

feature correlates with the minimum magnetic susceptibility value, while the maxima in susceptibility fall on the side slopes of the drainage feature. Susceptibility values along Line L (not shown) exhibit a similar variation to that in Fig. 4. However, Line M is slightly west of the major magnetic anomaly feature, and while the susceptibility values exhibit large variability (not shown), the same well-defined susceptibility pattern is not apparent. Also shown in Fig. 4 (and Table 1) are the results of laboratory measurements of magnetic susceptibility on 10-cm³ “remolded” soil samples from depths of 0.1, 0.5, and 1.0 m at locations K13, K7, and K1 (corresponding to Northing locations 100, 700, and 1300 ft, respectively).

The close correlation between the magnetic susceptibility variations and the magnetic anomaly itself strongly supports the shallow geologic origin of the magnetic anomaly. Results of a two-dimensional magnetic model calculation (Fig. 5) demonstrate that the general features of the observed magnetic anomaly can result from the observed magnetic susceptibility variations.

5.2. Northeast quadrant magnetic anomaly

Investigations of magnetic susceptibility variations in the northeast quadrant magnetic anomaly area were limited by close proximity to an active Phase IV demonstration area. Measurements were obtained with the MS2 system at 16 locations on a 30-m (100-ft) grid, bounded by the E, K, 1, and 4 lines. These measurements (not shown) indicate that within the lower elevation areas of the drainage features, susceptibility values are smaller by factors of 4 to 5 than values on the side slopes and higher elevations; this observation is consistent with the findings for the Northwest quadrant anomalous area.

5.3. Summary of JPG magnetic susceptibility measurements

A histogram of all magnetic susceptibility measurements at JPG is shown in Fig. 6. Although the data are not uniformly distributed over the 16-ha site, one obvious attribute is a peak at $\sim 3\text{--}4 \times 10^{-4}$ (SI),

Table 1
Magnetic susceptibilities for JPG soil samples

Location	Depth (m)	Magnetic susceptibility ($\times 10^{-5}$ SI)		%Frequency effect
		465 Hz	4650 Hz	
K1	0.1	73.6	67.3	8.6
	0.5	32.5	30.6	5.8
	1.0	17.2	16.4	4.6
K7	0.1	20.5	19.3	5.8
	0.5	15.1	13.8	8.6
K13	0.1	10.7	10.7	0
	0.5	14.8	14.6	1.4
	1.0	13.3	12.6	5.3
G1	0.1	62.9	58.7	6.7
	0.5	27.2	25.5	6.2
	1.0	28.2	26.7	5.3
G7	0.1	13.1	12.7	3.0
	0.5	7.1	6.9	2.8
G13	0.1	11.6	11.2	3.4
	0.5	8.8	8.1	8.6
	1.0	13.6	13.5	0.7
C1	0.1	65.3	62.1	4.9
	0.5	25.0	23.9	4.4
	1.0	31.5	30.3	3.8
C7	0.1	11.6	11.2	3.4
	0.5	9.0	8.8	2.2
	1.0	22.7	21.8	4.0
C13	0.1	19.9	19.9	4.0
	0.5	17.6	16.6	5.7
	1.0	21.5	20.9	2.8

which represents a peak in the background susceptibility distribution. Less definitive is the suggestion or possibility of a second peak at $\sim 9-10 \times 10^{-4}$, which represents the geologic anomaly areas. The overall shape is approximately that of a lognormal distribution commonly observed for numerous measurements in a relatively small area (Dearing, 1994). Table 1 contains the results of laboratory magnetic susceptibility measurements on “remolded” soil samples from three locations along each of three N–S lines, with two to three depths per location. Each value in Table 1 is the mean of measurements on three to six samples from each depth, and the susceptibility is determined at two frequencies (“low” frequency = 0.465 kHz and “high” frequency = 4.65 kHz).

6. Magnetic power spectral density considerations

One-dimensional, ensemble-averaged, total magnetic field profiles and power spectral density (PSD)

plots for three areas from the JPG site are shown in Fig. 7. The “Anomaly Region” plots (Fig. 7a and d) are for an area centered on the NW quadrant magnetic anomaly. The “Artillery/Mortar Site” (Fig. 7b and d) and “WES Site” (Fig. 7c and d) plots are for two representative “quiet” regions. Significantly, the Anomaly PSD curve for the anomaly region for k within the range $0.1 < k < 2$ cycles/m (cpm; includes most UXO magnetic signatures) is one to two orders of magnitude larger than either of the “quiet” region PSD curves. The peaks in all three curves for $k > 3$ cpm are caused by motion induced platform noise.

Khadr et al. (1999) compare PSDs for three sites (see Fig. 8), two very high-magnetic background sites on Maui, HI, and a quiet site at Fort Carson, CO (USA). The Fort Carson site magnetic background is comparable to the JPG quiet sites in Fig. 7, and UXO signatures are detectable as a bulge relative to a line representing the geologic background with the ubiquitous $1/k^2$ slope. For the Maui sites, the PSDs are two orders of magnitude larger than even the JPG “Anomaly” site in Fig. 7. At the Maui sites, even magnetic signatures of very large UXO (e.g., 2000-lb bombs) are not discernable relative to the background, and the slope of the spectral curve is closer to $1/k^3$.

7. Summary and conclusions: implications of background magnetic susceptibility for UXO detection and general approaches for data processing and interpretation

The magnetic susceptibility variations over the 40-acre site at JPG pose location-specific problems for UXO detection with total magnetic field surveys. Model calculations and laboratory measurements of TFM response for ferrous metallic objects indicate that the results are relatively insensitive to the value of relative susceptibility of the steel of the ordnance item, once it is large enough (>150 , which holds for most steels; McFee and Das, 1990). For conditions at sites like JPG, the ferrous metallic ordnance to surrounding material contrast in relative magnetic susceptibility is as small as 10^5 in the geologic anomaly areas, whereas the contrast in electrical conductivity is $>10^7$ everywhere. Even though the magnetic susceptibility contrast between ordnance and geologic materials at JPG is still large, detection of ordnance objects

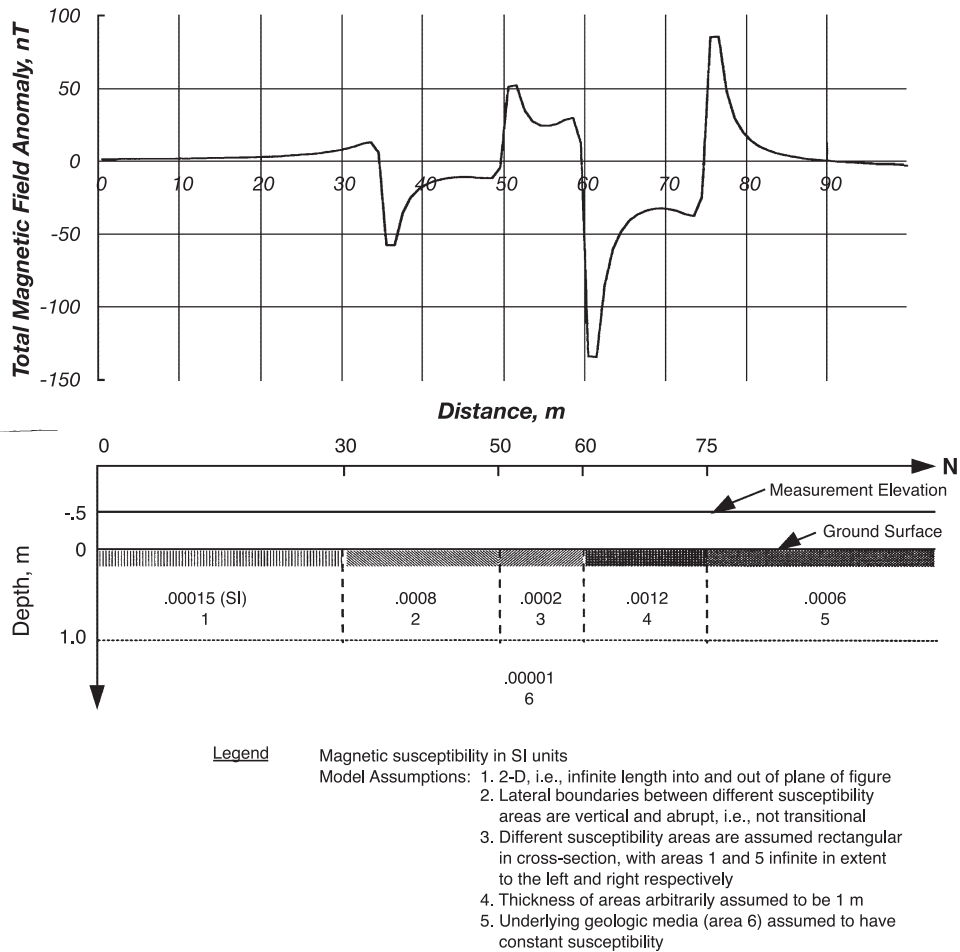


Fig. 5. Total magnetic field calculation for hypothetical, two-dimensional model approximation of magnetic susceptibility based on measurements along the K-line at the JPG site (Fig. 4).

becomes problematic when buried in “large volume” (pervasive) magnetic susceptibility contrast areas, which can mask the volume-dependent anomaly caused by the UXO. For volcanic terrains such as Kaho’olawe and Maui, HI, the relative magnetic susceptibility contrast is as small as 10^3 – 10^4 everywhere (see Table 2). Thus the signal to noise ratio is small ($S/N < 1$) for most buried ordnance items in sites like Kaho’olawe and Maui, and UXO detection with TFM is problematic everywhere (Khadr et al., 1997). Localized magnetic susceptibility anomalies (e.g., JPG) and high susceptibility backgrounds can also contribute to poor GPR and TDEM performance.

Examination of high-resolution, high-accuracy total magnetic field anomaly maps of the 40-acre site at

JPG (Butler et al., 1999) reveals that the magnetic background (noise level) areas of the 40-acre site vary from “quiet” ($< \pm 5$ nT) to noisy ($\sim \pm 20$ nT) to anomalous (> 100 nT). The model-predicted total magnetic field anomalies for the Phase II and III baseline ordnance items (ordnance items buried for the demonstrations; see Fig. 9, where the bars indicate the range of burial depths for each ordnance item) indicates that the *minimum* peak positive anomaly magnitude for Phase III is 18 nT, while some Phase II baseline ordnance targets have anomaly values < 10 nT. For the magnetically quiet areas of the site, only a small number of the Phase II baseline ordnance targets are problematically detectable. For magnetically noisy areas of the site, however, a small number of Phase III

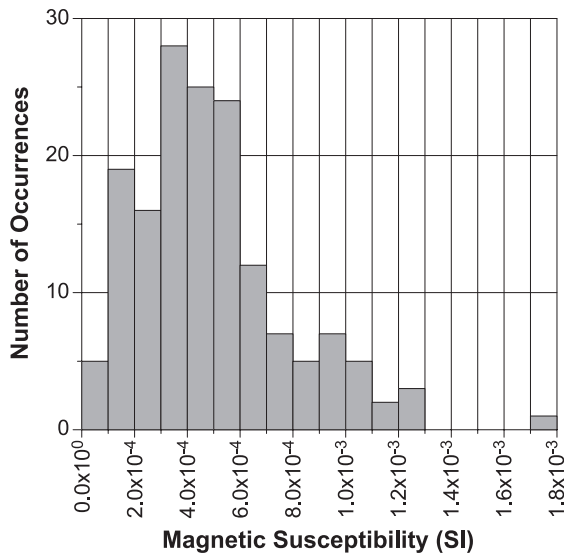


Fig. 6. Histogram of JPG susceptibility values.

ordnance targets and a significant number of Phase II targets become problematically detectable. In the northwest quadrant anomalous area, a significant number of ordnance items from all the demonstration phases are problematically detectable (Butler et al., 1999).

7.1. TFM

For sites with high magnetic background everywhere, e.g., Kaho'olawe, the approach is simply not to rely on TFM for UXO detection. Sites like JPG with highly variable magnetic backgrounds, from quiet to noisy to prominent geologic anomalies, the approaches must vary. Quiet sites allow efficient UXO detection with TFM, and the complete definition of the UXO magnetic anomalies offers the potential for discrimination and identification (e.g., Billings et al., 2002a,b,c). For sites with magnetic backgrounds that can interfere with UXO detection but not so pervasively large in magnitude as to mask UXO anomalies, approaches must be tailored to the spatial characteristics of the background. The approaches include:

- data filtering in the wavenumber domain, e.g., notch filters designed to retain wavenumbers in a range covering the ordnance items expected at the site,

e.g., the range ~ 0.04 – 2 cpm will cover virtually all ordnance;

- *measure* a finite interval vertical gradient, with the lower sensor height and the sensor interval chosen based on the depth ranges of interest (e.g., Butler, 1984); alternatively, *compute* the vertical gradient from closely spaced TFM measurements using a discrete, generalized Hilbert transform (Nabighian and Hansen, 2001)
- upward continue by small distance to attenuate anomalies caused by small surface and very shallow ferrous objects (clutter, such as shown in Fig. 2b);
- use a moving window, high-pass median filter to remove geologic background components below a pre-determined maximum depth of interest (Billings et al., 2002b; Kilty, 1999; Evans, 1982); similarly, a moving window, low-pass median filter will act as a despiker to remove instrument spikes or very short wavelength signals due to small surface/very shallow ferrous clutter (Evans, 1982).

These general approaches to processing TFM data are well established. For UXO detection and discrimination applications, the goal is to preserve the maximum information content in anomalies from sources in the depth range of interest to UXO detection and discrimination. Often, two or more of these approaches will be combined, e.g., application of a high-pass median filter followed by a small-distance upward continuation (Billings et al., 2002b). UXO detection is commonly achieved in noisy settings like some of the areas at JPG, but capability to discriminate and identify will be degraded. The degradation results from anomaly superposition and/or partial masking of anomalies by the magnetic background.

7.2. TDEM

For TDEM the implications of magnetic backgrounds are different than for TFM, due to different magnetic phenomenology. For TFM, the inducing field is static, i.e., not time- or frequency-dependent, and the magnetic susceptibility and magnetization are constant. With FDEM or TDEM systems, frequency dependence of the magnetic susceptibility (complex quantity) of the soil may affect the anomaly response. A frequency-dependent magnetic susceptibility for the

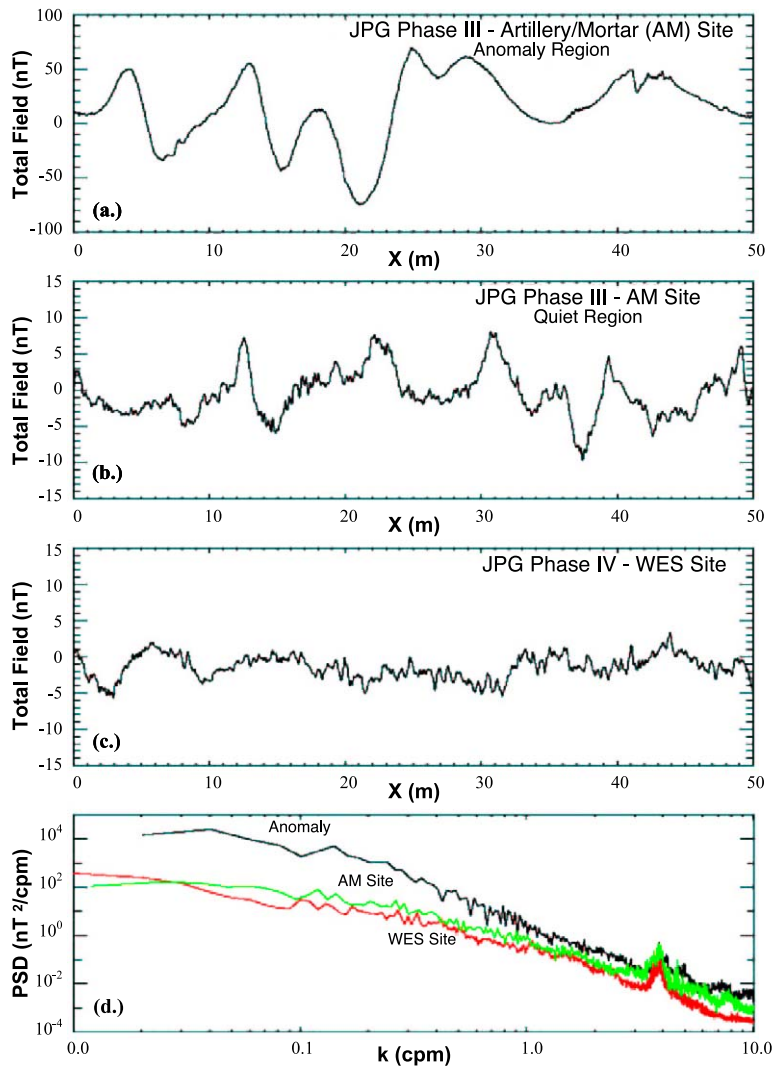


Fig. 7. Ensemble average of magnetic field along measurement lines for three regions at the JPG site (a–c) and power spectral density (PSD) for the three regions (d); note difference in vertical scale between a and b–c.

soil results in a time-dependent rotation of the magnetization vector to align with the inducing field. The rotation can be characterized by a time constant for the magnetization to rotate from its minimum energy position before and after application of the inducing field. This time-dependent phenomenon is known as magnetic viscosity; and for a soil with magnetic grains that have a large range of relaxation times that are uniformly distributed over their spectrum, the time derivative of the induced magnetic field decays as t^{-1} (Chikazumi, 1997; Pasion et al., 2002, 2003). The t^{-1}

decay for a “magnetic soil”, with frequency-dependent susceptibility, contrasts to the commonly observed $t^{-5/2}$ decay for soil with real, constant susceptibility (Kaufman and Keller, 1983; Butler and Fitterman, 1986).

While UXO can be detected even in the presence of soils with pervasive, large, frequency-dependent magnetic susceptibility (Khadri et al., 1997), problems arise in attempting to invert the TDEM anomaly data for target characteristics (discrimination and identification). Such conditions exist at Kaho’olawe Island,

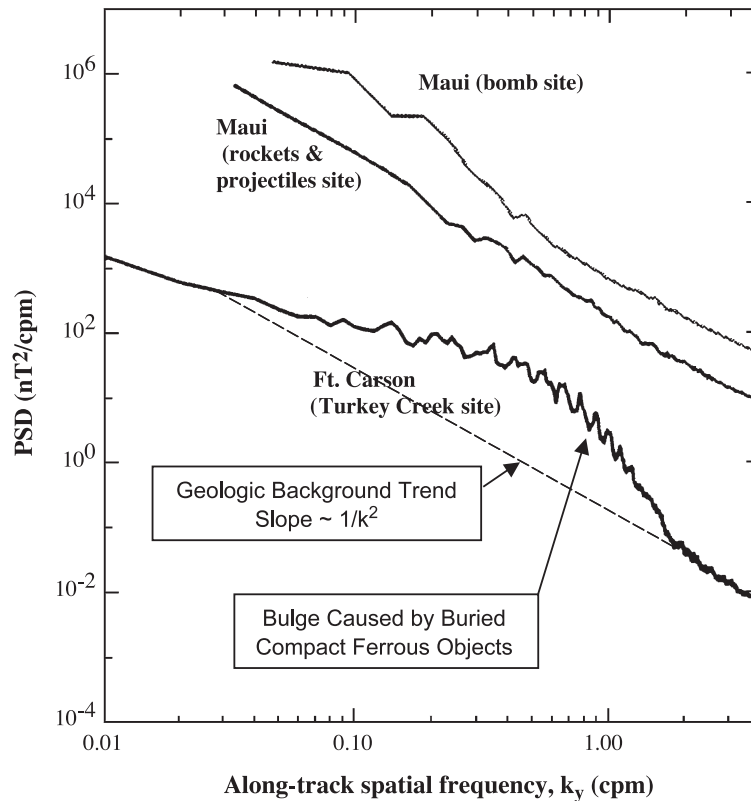


Fig. 8. Comparison of ensemble average PSDs for three sites. The Ft. Carson site is magnetically “quiet”, and the bulge and peaks from ~ 0.04 to 2 cpm is due to buried ordnance and other ferrous items.

HI, for example. Comparing the magnetic susceptibility data in Table 2 for Kaho’olawe with the data in Table 1 for JPG indicates the JPG susceptibilities have similar, though more variable, frequency dependence; however, JPG susceptibilities are nominally two orders of magnitude smaller than Kaho’olawe.

Pasion et al. (2002, 2003) consider both the Lee model (Lee, 1983) and the Cole–Cole model (e.g., Olhoeft and Strangway, 1974; Dubas et al., 1992) and show that the “magnetic soil” response can be characterized by the expression $F=At^{-1}$ over the time range of interest for UXO survey applications. The parameter A controls the overall magnitude of the soil response. Pasion et al. (2002, 2003) demonstrate how data such as in Tables 1 and 2 can be used to fit a model of the frequency-dependent susceptibility and calculate the response parameter A .

Ability to recover the characteristics of buried metallic objects by inversion of TDEM data depends

on the value of A . For $A=0$ (“nonmagnetic soil”), TDEM inversion is limited only by basic signal to noise considerations, e.g., can the ordnance item be detected, and if so, can the time decay signature and spatial signature be determined relative to background and instrument noise levels. Further, Pasion et al. demonstrate for a particular ordnance item buried in a frequency-dependent soil that inversion for model parameters is reasonably successful for $A=50$ mV but not for $A=100$ mV. This research is ongoing, but preliminary results suggest an approach for removing the effects of the magnetic soil response to enhance data inversion. The approach for background removal requires that the background response be determined in areas where the response does not include the effects of buried metallic objects. For TDEM systems with three-component receivers, the process is simplified since the horizontal components of the background soil response are zero due to symmetry (i.e.,

Table 2
Magnetic susceptibilities from selected locations at two sites on Kaho’olawe Island, HI

Sample no./depth (m)	Magnetic susceptibility ($\times 10^{-5}$ SI)		
	Low frequency (0.46 kHz)	High frequency (4.6 kHz)	%Frequency effect
<i>Site Seagull</i>			
7462–2728 A—0.15	3554	3311	7.0
7462–2728 A—0.61	3022	2771	8.2
7462–2728 B—0.15	1046	1001	4.3
7468–2734 A-P—0.15	1726	1630	5.6
7468–2734 A-P—0.46	1529	1448	5.3
7468–2734 B-P—0.30	2807	2634	6.2
7468–2734 B-P—0.46	1920	1807	5.9
7468–2734 A-B—0.15	845	805	4.6
7468–2734 B-B—0.20	1795	1707	4.9
<i>Site Lua Kakika</i>			
7537–2754 A-P—0.20	2355	2249	4.5
7537–2754 A-P—0.46	2227	2134	4.2
7537–2754 B-P—0.15	1461	1383	5.4
7537–2754 B-P—0.30	1497	1411	5.8
7537–2754 A-B—0.15	2475	2431	1.8
7537–2754 B (Back)—0.30	1394	1334	4.3

the frequency-dependent susceptibility of soil that is nominally pervasive laterally affects only the vertical component due to symmetry). Thus plots of the mean

square magnitude of the horizontal component can be used (1) for enhanced detection, (2) to select locations free of anomalous response due to buried objects, and (3) to fit the vertical component time decay at those locations to obtain $F = At^{-1}$. Then, using a representative or mean value of A from the surrounding decay time fits, subtract the At^{-1} response from signatures in anomalous areas over buried objects.

7.3. General

Once the detailed nature of the magnetic background of sites is known, decisions regarding application of geophysical surveys for detection and discrimination of UXO are possible. General approaches and guidelines for analyzing site characterization data and processing survey data are indicated above. However, the greater issue is how to predict appropriate approaches for potentially UXO-contaminated sites in advance or from a minimum amount of site characterization information. Current research addresses this greater issue, using existing site information (soil maps, topographic maps, vegetation maps, remote imagery, etc.), site characterization (limited) geophysical surveys, and soil sampling. Soil sampling allows soils classification (mineralogy, par-

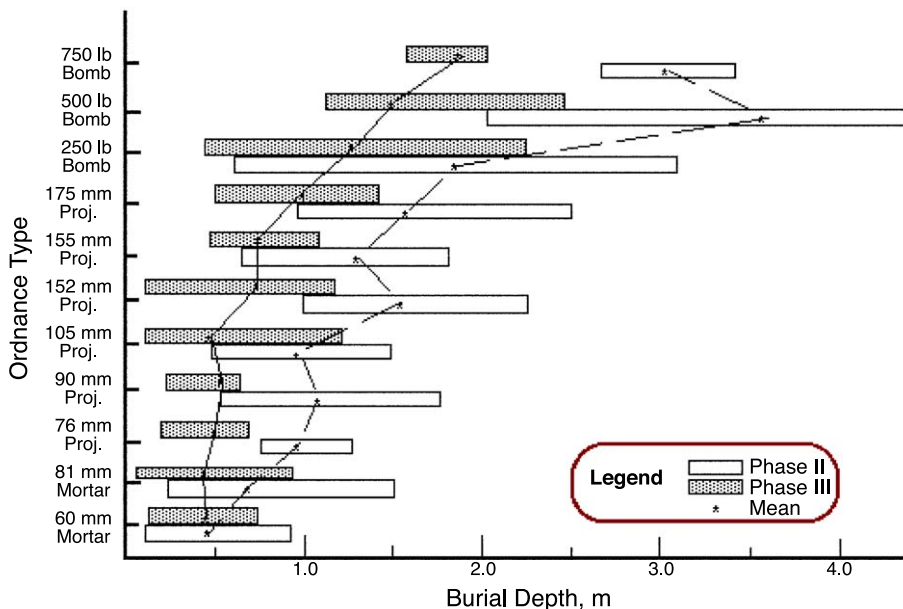


Fig. 9. Comparison of ordnance burial depths for JPG Phase II and III.

ticle size gradation) and direct soil property measurements. A fundamental issue currently under investigation is the nature of frequency-dependent magnetic susceptibility and its effect on TDEM surveys. Another fundamental issue relates to the existence, nature and magnitude of remanent magnetization of intact UXO and UXO fragments; current approaches to UXO discrimination using TFM involve assumptions about remanent magnetization.

Acknowledgements

This paper results from work conducted as part of the UXO Focus Area of the U.S. Army's Environmental Quality Technology Research Program by personnel of the U.S. Army Engineer Research and Development Center (ERDC) and Alion Science and Technology Corporation. The author has freely drawn from superb work done by personnel of the Geophysical Inversion Facility, University of British Columbia (UBC), funded by ERDC. ERDC personnel who contributed to this work include Janet Simms, Jose Llopis, and Eric Smith; UBC personnel including Douglas Oldenburg, Len Pasion, and Stephen Billings. The author also gratefully acknowledges discussions with Nagi Khadr and Bruce Barrow, AETC, and their assistance in developing Fig. 7. The paper, in its final form, benefited significantly from constructive reviews of the original paper by Dr. Alain Tabbaugh and a second reviewer.

References

- Billings, S.D., Pasion, L.R., Oldenburg, D.W., 2002a. Discrimination and Identification of UXO by Geophysical Inversion of Total-Field Magnetic Data, Technical Report ERDC/GSL TR-02-16, U.S. Army Engineer Research and Development Center, Vicksburg, MS.
- Billings, S.D., Stanley, J.M., Youmans, C., 2002b. Magnetic discrimination that will satisfy regulators. Proceedings of the UXO/Countermine Forum 2002 (CD), Orlando, FL.
- Billings, S.D., Pasion, L.R., Oldenburg, D.W., 2002c. UXO discrimination and identification using magnetometry. Proceedings of the Symposium on the Application of Geophysics to Environmental and Engineering Problems (CD). Environmental and Engineering Geophysical Society, Las Vegas, NV.
- Burger, H.R., 1992. Exploration Geophysics of the Shallow Subsurface. Prentice Hall, Englewood Cliffs, NJ.
- Butler, D.K., 1984. Interval gravity gradient determination concepts. *Geophysics* 49, 828–832.
- Butler, D.K., 1997. Round table: landmines and UXO. *The Leading Edge* 16 (10), 1460.
- Butler, D.K., 2001. Potential fields methods for location of unexploded ordnance. *The Leading Edge* 20 (8), 890–895.
- Butler, D.K., Fitterman, D.V., 1986. Transient electromagnetic methods for ground-water assessment, Miscellaneous Paper G-86-27, US Army Engineer Waterways Experiment Station, Vicksburg, MS.
- Butler, D.K., Cespedes, E.R., Cox, C.B., Wolfe, P.J., 1998a. Multisensor methods for buried unexploded ordnance detection, discrimination, and identifications, Technical Report SERDP-98-10, US Army Engineer Waterways Experiment Station, Vicksburg, MS.
- Butler, D., Cespedes, E., O'Neill, K., Arcone, S., Llopis, J., Curtis, J., Cullinane, J., Meyer, C., 1998b. Overview of science and technology program for JPG phase IV. Proceedings of the UXO Forum '98, Anaheim, CA.
- Butler, D.K., Llopis, J.L., Simms, J.E. 1999. Phenomenological Investigations of the Jefferson Proving Ground UXO Technology Demonstrations, Technical Report GL-99-7, U.S Army Engineer Waterways Experiment Station, Vicksburg, MS.
- Butler, D.K., Wolfe, P.J., Hansen, R.O., 2001. Analytical modeling of magnetic and gravity signatures of unexploded ordnance. *Journal of Environmental and Engineering Geophysics* 6 (1), 33–46.
- Cespedes, E.R., 2001. Advanced UXO detection/discrimination technology demonstration—U.S. Army Jefferson Proving Ground, Madison, Indiana, Technical Report ERDC/EL TR01-1, Engineer Research and Development Center, Vicksburg, MS.
- Cespedes, E.R., Dinh, H.Q., 2002. Performance of advanced EMI systems in difficult magnetic environments. Proceedings of the UXO/Countermine Forum 2002, Orlando, FL.
- Chikazumi, S., 1997. *Physics of Ferromagnetism* Oxford University Press, New York.
- Dearing, J., 1994. *Environmental Magnetic Susceptibility Using the Bartington MS2 System* Chi Publishing, Kenilworth, UK.
- Dubas, M., Jolivet, J., Tabbaugh, A., 1992. Magnetic susceptibility and viscosity of soils in a weak time varying field. *Geophysical Journal International* 108, 101–109.
- Evans, J.R., 1982. Running median filters and a general despiker. *Bulletin of the Seismological Society of America* 72 (1), 331–338.
- Kaufman, A.A., Keller, G.V., 1983. *Frequency and Transient Soundings* Elsevier, New York.
- Keiswetter, D., 2000. Advances in frequency domain electromagnetic induction techniques for improved discrimination and identification of buried unexploded ordnance. Proceedings of the UXO/Countermine Forum 2000, Anaheim, CA.
- Khadr, N., Bell, T., William, S., Bacon, W.B., 1997. UXO detection in highly magnetic soils. Proceedings of the UXO Forum 97, 222–228.
- Kilty, K.T. 1999. Filtering magnetic data to remove cultural noise. <http://www.kilty.com/filter.htm>, ©1999, 13 pages (7 June 2002).
- Le Borgne, E., 1955. Abnormal magnetic susceptibility of the top soil. *Annals of Geophysics* 11, 399–419.

- McDonald, J.R., Nelson, H.H., 1999. Results of the MTADS Technology Demonstration #3 Naval Research Laboratory, Washington, DC. NRL/PU/6110-99-375.
- McFee, J.E., Das, Y., 1990. A multiple expansion model for compact ferrous object detection. Proceedings of the ANTEM '90 Symposium on Antenna Technology and Applied Electromagnetics, Manitoba, Canada, 633–638.
- McNeill, J.D., 1986. Geonics EM38 Ground Conductivity Meter, Operating Instructions and Survey Interpretation Techniques, Technical Note TN-21, Geonics, Mississauga, Ontario, Canada.
- Mullins, C.E., 1977. Magnetic Susceptibility of the soil and its significance in soil science a review. *Journal of Soil Science* 28, 223–246.
- Nabighian, M.N., Hansen, R.O., 2001. Unification of Euler and Werner deconvolution in three dimensions via the generalized Hilbert transform. *Geophysics* 66, 1805–1810.
- Olhoeft, R.R., Strangway, D.W., 1974. Magnetic relaxation and the electromagnetic response parameter. *Geophysics* 39, 302–311.
- Pasion, L.R., Oldenburg, D.W., 2001. A discrimination algorithm for UXO using time domain electromagnetics. *Journal of Engineering and Environmental Geophysics* 6 (2), 91–102.
- Pasion, L.R., Billings, S.D., Oldenburg, D.W., 2002. Evaluating the effects of magnetic soils on TEM measurements for UXO detection. Expanded Abstracts. Society of Exploration Geophysicists, Tulsa, OK, pp. 1428–1431.
- Pasion, L.R., Billings, S.D., Oldenburg, D.W., 2003. Evaluating the effects of magnetic susceptibility in UXO discrimination problems. Proceedings of the Symposium on the Application of Geophysics to Environmental and Engineering Problems (CD). Environmental and Engineering Geophysical Society, San Antonio, TX.
- Pederson, A., Stalcup, B., 1997. Phase III advanced technology demonstrations at Jefferson proving ground. Proceedings of the UXO Forum '97, pp. 281–289.
- Scollar, I., Tabbagh, A., Hesse, A., Herzog, I., 1990. *Archaeological Prospecting and Remote Sensing* Cambridge Univ. Press, NY.